THE MAGNETO-ELASTIC INTERNAL RESONANCES OF RECTANGULAR CONDUCTIVE THIN PLATE WITH DIFFERENT SIZE RATIOS

J. Li

Key Laboratory of Mechanical Reliability for Heavy Equipment and Large Structures of Hebei Province
Yanshan University
Qinhuangdao, China

Department of Basic Teaching
Tangshan University
Tangshan, China

Y. D. Hu*

Key Laboratory of Mechanical Reliability for Heavy Equipment and Large Structures of Hebei Province
Yanshan University
Qinhuangdao, China

Y. N. Wang

School of Engineering
Deakin University
Waurn Ponds campus
Geelong, Australia

ABSTRACT

Based on the basic equations of electromagnetic elastic motion and the expression of electromagnetic force, the electromagnetic vibration equation of the rectangular thin plate in transverse magnetic field is obtained. For a rectangular plate with one side fixed and three other sides simply supported, its time variable and space variable are separated by the method of Galerkin, and the two-degree-of-freedom nonlinear Duffing vibration differential equations are proposed. The method of multiple scales is adopted to solve the model equations and obtain four first-order ordinary differential equations governing modulation of the amplitudes and phase angles involved via 1:1 or 1:3 internal resonances with different size ratios. With a numerical example, the time history response diagrams, phase portraits and 3-dimension responses of two order modal amplitudes are respectively captured. And the effects of initial values, thickness and magnetic field intensities on internal resonance characteristics are discussed respectively. The results also present obvious characteristics of typical nonlinear internal resonance in this paper.

Keywords: Magneto elastic, Rectangular conductive thin plate, Internal resonance, Multiple-scale.

1. INTRODUCTION

With the rapid development of modern science and technology, the electromagnetic structures have been widely used in many high-tech devices and equipment, such as in aerospace, MAGLEV transportation, electro-mechanical dynamical system and large water conservancy and hydropower projects. The research on the theory of electromagnetic elastic mechanics and its applications have attracted considerable attention. While the research of magneto elastic dynamics in electromagnetic field has important theoretical and practical significance [1]. Many researchers have been paying much attention on mechanical behavior in magnetic field of a conductive thin rectangular plate or shell, as a typical structure. Zheng *et al*. analyzed the dynamic stability of the cantilever conductive thin plate in the transverse pulsed magnetic field [2] and a theoretical model for soft ferromagnetic shells was derived to describe their magneto-elastic behavior in a magnetic field with

* Corresponding author (huyuda03@163.com)

DOI : 10.1017/jmech.2017.30
Copyright © 2017 The Society of Theoretical and Applied Mechanics
https://doi.org/10.1017/jmech.2017.30 Published online by Cambridge University Press

the aid of a generalized variational method [3]. The fundamental equations of the ferromagnetic beam-plate including magneto-elastic interaction and magnetic damping were derived and the dynamic stability of a soft ferromagnetic beam-plate in a transverse magnetic field was also investigated [4]. Pratiher *et al*. [5] proposed the temporal equation of motion of the system containing linear and nonlinear parametric excitation terms along with nonlinear damping, geometric and inertial types of nonlinear terms and solved the equations by using method of multiple scales. The stability and bifurcation analysis of a cantilever beam subject to periodically varying axial load and magnetic field for three different resonance conditions were explored [6]. The nonlinear magneto elastic vibration equations of conductive thin plate in the transverse magnetic field was given, and the complex dynamics and stability of the system under sub harmonic resonance and combination resonance were analyzed in [7-9]. Hu *et al*. [10] derived the strongly nonlinear sub-harmonic resonance bifurcation-response equations of the strip thin plate in transverse magnetic field by using improved multiple-scale method. They analyzed the influences of different bifurcation parameters on periodic motion, periodic time motion, and chaotic motion behaviors of sub-harmonic resonance system. Hamilton's variational principle was applied to derive the nonlinear magneto thermo-elastic coupling vibration equation of the axially moving conductive plate by the interaction of force, motion, electric, magnetic and thermal effects [11].

For MDOF system, when the parameters of the system change to make some natural frequencies of the system commensurable or nearly commensurable, the mutual interference between different modes of vibration will occur. The modal interference between modes will lead to energy exchange, and the energy transfer only occurs between the interferential modes. It is the inherent characteristics of vibration system under certain parameters, which is internal resonance. Internal resonance can exist in many mechanical systems, including beams, plates, shells, etc. A large number of theoretical and experimental studies have shown that the internal resonance establishes an energy exchange mechanism between the modes of a MDOF nonlinear vibration system and makes the modes coupling possible [12]. Internal resonance is also one of the unique phenomena in nonlinear vibration which are distinct from linear vibration. These have been added in the introduction. Witt and Gorelik [13] were among the first to show theoretically and experimentally the two-to-one internal resonance with the energy exchange from one subsystem to another using the simplest two-degree-of-freedom mechanical system as an example, research interest to the problem of the internal resonance in mechanical systems has always been strong. Chen *et al*. [14] analyzed the effects of forced vibration on the steady state response of a coupled cantilever beam system under nonlinear boundary conditions in the presence of 2:1 internal resonance. The method of multiple scales was utilized to investigate nonlinear vibration of a rectangular metal plate of simply supported [15] or a composite laminated cantilever rectangular plate [16] under 1:1 internal resonance and external excitation. Li *et al*. [17] used the generalized Melnikov method for the first time to study the global bifurcation and multi pulse dynamics of rectangular plate which is subject to transversal and in-plane excitation with four edges simply supported under 1:1 internal resonance. The nonlinear dynamic responses of functionally graded rectangular plate and a viscoelastic plate were investigated under the conditions of different internal resonances [18-19]. Nayfeh *et al*. [20] applied the method of multiple scales to derive the modulation equations about the amplitudes and phase angles of buckling beam under 1:1 and 1:3 internal resonance conditions. The equilibrium solutions of the modulation equations were obtained and their stability was also investigated. The dynamic responses of the axially moving beam with the dual frequency parameter excitation under the condition of combined resonance, primary parametric resonance and internal resonance were analyzed by Sahoo *et al*. [21]. The 3:1 internal resonance of multiple stepped beam with cubic nonlinearities was analyzed by the method of multiple scales [22]. Xiong *et al*. [23] studied the nonlinear dynamics of a viscoelastic buckled beam subject to primary resonance in the presence of 2:1 internal resonance for the first time. The unstable regions in the internal resonance were explored via numerical simulation. From the review of literature, it is found that there are many studies about the magneto elastic vibration and internal resonance of the beam, plate and shell, but the investigation of the conductive plate in the magnetic field via internal resonance has not been explored yet.

The objective of this study is to investigate the internal resonance characteristics of rectangular conductive thin plate with different size ratios. The nonlinear magneto elastic vibration equation is derived for rectangular thin conductive plate with one side fixed and three other sides simply supported in a constant magnetic field. The method of multiple scales is utilized to obtain four non-linear ordinary-differential equations governing modulation of the amplitudes and phase angles of the interacting modes under different internal resonance conditions. We also analyze the internal resonance characteristics via the time history response diagrams, phase diagrams and 3-dimension responses of two order modal amplitudes.

2. MAGNETO-ELASTIC BASIC EQUATIONS OF RECTANGULAR CONDUCTIVE PLATE

2.1 Electro-Dynamic Equations and Expressions of Electromagnetic Forces

Considering the non-polarized, non-magnetic and highly conductive material, we establish the Cartesian coordinate system $Oxyz$ in magnetic field (xy is the middle plane of the plate and z is along the normal direction of the middle plane) as shown in Fig. 1. The electromagnetic constitutive relation of electromagnetic parameters can be obtained by the Maxwell's electromagnetic equation

https://doi.org/10.1017/jmech.2017.30 Published online by Cambridge University Press

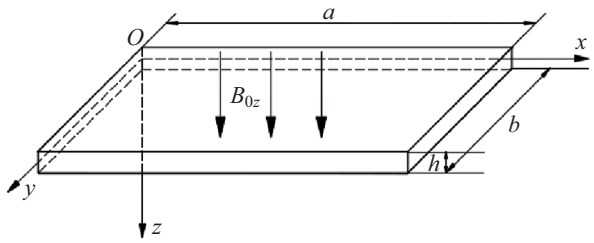


Fig. 1 Conductive thin plate in a transverse magnetic field.

$$\boldsymbol{J}=\sigma\left(\boldsymbol{E}+\frac{\partial \boldsymbol{u}}{\partial t}\times\boldsymbol{B}\right) \tag{1}$$

The vector expression of the Lorenz force is [1]

$$\boldsymbol{f}(f_x,f_y,f_z)=\boldsymbol{J}\times\boldsymbol{B} \tag{2}$$

where $\boldsymbol{B}(B_x,B_y,B_z)$ is the magnetic induction vector, $\boldsymbol{J}(J_x,J_y,J_z)$ is the conduction current-density vector, $\boldsymbol{E}(E_x,E_y,E_z)$ is the electric field vector, $\boldsymbol{u}(u_x,u_y,u_z)$ is the displacement vector of each internal point of the conductor, σ is the electrical conductivity, and t is time variable.

With Eq. (1) and according to the electromagnetic elastic hypothesis and the linearization method of thin plates and shells [1], we ignore the electromagnetic parameter excited by disturbance and the higher order items of elastic displacements, so the expressions of electromagnetic force and moment in a unit area of thin plate are obtained

$$F_z=\sigma hB_{0y}\left(e_x-B_{0y}\frac{\partial w}{\partial t}+B_{0z}\frac{\partial v}{\partial t}\right)$$
$$-\sigma hB_{0x}\left(e_y+B_{0x}\frac{\partial w}{\partial t}-B_{0z}\frac{\partial u}{\partial t}\right)=0 \tag{3-1}$$

$$m_x=\frac{\sigma h^3}{12}B_{0z}^2\frac{\partial^2 w}{\partial t\partial x} \tag{3-2}$$

$$m_y=\frac{\sigma h^3}{12}B_{0z}^2\frac{\partial^2 w}{\partial t\partial y} \tag{3-3}$$

where $\boldsymbol{e}(e_x,e_y,e_z)$ is electric field intensity vector, u, v, w represent the displacement component of the middle plane about x, y, z axis respectively.

2.2 The Nonlinear Magneto-Elasticity Vibration Equation

We consider the thin rectangular conductive plate in an external transverse magnetic field as Fig. 1 shown. According to the Von Karman large deflection bending theory, the plane geometric equations are given by

$$\varepsilon_x=\frac{\partial u}{\partial x}+\frac{1}{2}\left(\frac{\partial w}{\partial x}\right)^2,\quad \varepsilon_y=\frac{\partial v}{\partial y}+\frac{1}{2}\left(\frac{\partial w}{\partial y}\right)^2,$$
$$\gamma_{xy}=\frac{\partial u}{\partial y}+\frac{\partial v}{\partial x}+\frac{\partial w}{\partial x}\frac{\partial w}{\partial y},\quad \kappa_x=-\frac{\partial^2 w}{\partial x^2},$$
$$\kappa_y=-\frac{\partial^2 w}{\partial y^2},\quad \kappa_{xy}=-\frac{\partial^2 w}{\partial x\partial y} \tag{4}$$

The physical equations are given by

$$N_x=D_N(\varepsilon_x+\nu\varepsilon_y),\quad N_y=D_N(\varepsilon_y+\nu\varepsilon_x),$$
$$N_{xy}=D_N\left(\frac{1-\nu}{2}\right)\gamma_{xy},\quad M_x=D_M(\kappa_x+\nu\kappa_y),$$
$$M_y=D_M(\kappa_y+\nu\kappa_x),\quad M_{xy}=D_M(1-\nu)\kappa_{xy} \tag{5}$$

Based on Kirchhoff's fundamental assumption and accounting for the coupling effect of mechanical field and electromagnetic field, we can obtain the nonlinear magneto-elastic vibration equation of a conductive thin plate according to the principle of virtual work while ignoring the effect of inertia force in middle surface as follows [7]

$$\frac{\partial^2 M_x}{\partial x^2}+\frac{\partial^2 M_y}{\partial y^2}+2\frac{\partial^2 M_{xy}}{\partial x\partial y}+\frac{\partial}{\partial x}\left(N_x\frac{\partial w}{\partial x}+N_{xy}\frac{\partial w}{\partial y}\right)$$
$$+\frac{\partial}{\partial y}\left(N_y\frac{\partial w}{\partial y}+N_{xy}\frac{\partial w}{\partial x}\right)+\frac{\partial m_x}{\partial x}+\frac{\partial m_y}{\partial y}+F_z+P_z$$
$$=\rho h\frac{\partial^2 w}{\partial t^2} \tag{6}$$

where N_x, N_y, N_{xy} are in-plane forces, M_x, M_y, M_{xy} are bending moments, P_z is mechanical load, F_z is electromagnetic force, m_x, m_y are electromagnetic moments, ρ is the density of the material, h is the thickness of thin plate and t is time variable.

Substituting the geometric equations and physical equations into vibration equation (6), the nonlinear magneto elastic vibration differential equation which is only about w under the conditions of no external excitation and constant transverse magnetic field is derived as follows

$$-D_M\nabla^4 w+\frac{D_N}{2}\left[3\left(\frac{\partial w}{\partial x}\right)^2\frac{\partial^2 w}{\partial x^2}+3\left(\frac{\partial w}{\partial y}\right)^2\frac{\partial^2 w}{\partial y^2}\right.$$
$$\left.+4\frac{\partial w}{\partial x}\frac{\partial w}{\partial y}\frac{\partial^2 w}{\partial x\partial y}+\left(\frac{\partial w}{\partial y}\right)^2\frac{\partial^2 w}{\partial x^2}+\left(\frac{\partial w}{\partial x}\right)^2\frac{\partial^2 w}{\partial y^2}\right]$$
$$+\frac{\sigma h^3B_{0z}^2}{12}\frac{\partial}{\partial t}\left(\frac{\partial^2 w}{\partial x^2}+\frac{\partial^2 w}{\partial y^2}\right)-\rho h\frac{\partial^2 w}{\partial t^2}=0 \tag{7}$$

where $D_N=\dfrac{Eh}{1-\nu^2}$ is the tensile stiffness, $D_M=\dfrac{Eh^3}{12(1-\nu^2)}$ is the flexural stiffness, E is the Young's modulus, ν is the Poisson's ratio and the differ-

https://doi.org/10.1017/jmech.2017.30 Published online by Cambridge University Press

ential operator is $\nabla^4 = \frac{\partial^4}{\partial x^4} + 2\frac{\partial^4}{\partial x^2 \partial y^2} + \frac{\partial^4}{\partial y^4}$.

3. SOLUTIONS OF 1:1 AND 1:3 INTERNAL RESONANCES

3.1 Vibration Differential Equations

The internal resonance of nonlinear systems is that there are positive or negative integers n_1, n_2, …, n_n that can make a number of system's natural frequencies ω_1, ω_2, …, ω_n satisfy the following relationship

$$n_1\omega_1 + n_2\omega_2 + \cdots + n_n\omega_n \approx 0 \tag{8}$$

The vibration system with internal resonance is very common and is also one of the special phenomena of the nonlinear vibration that distinguish from the linear vibration.

Considering the rectangular thin plate with one side fixed and the other three sides simply supported, the boundary conditions are

$$x = 0, \quad w = \frac{\partial w}{\partial x} = 0; \quad x = a, \quad w = \frac{\partial^2 w}{\partial x^2} = 0;$$
$$y = 0, \quad w = \frac{\partial^2 w}{\partial x^2} = 0; \quad y = b, \quad w = \frac{\partial^2 w}{\partial x^2} = 0.$$

Considering the first and the second modals and using dissociation variable method to separate the time and space variables, the displacement solutions which satisfy the boundary conditions can be expressed as follows [24]:

$$w(x,y,t) = \sum_{n=1}^{2} P_n(t) X_n(x) \sin\frac{\pi y}{b} \tag{9}$$

where $X_n = \cosh\beta_n x - \cos\beta_n x - C_n(\sinh\beta_n x - \sin\beta_n x)$,

$C_n = \frac{\cosh\beta_n a + \cos\beta_n a}{\sinh\beta_n a + \sin\beta_n l}$, $\beta_n = \frac{(4n+1)\pi}{4a}$.

Substituting Eq. (9) into Eq. (7), by using the Galerkin integral method the non-dimensional vibration differential equations of rectangular thin plate can be derived as

$$\begin{aligned}&\ddot{q}_1(t) + \omega_1^2 q_1(t) = -\varepsilon g_1^2 q_2(t) + \varepsilon c_{11}\dot{q}_1(t)\\&+\varepsilon c_{21}\dot{q}_2(t) + \varepsilon\left[\eta_{11}q_1^3(t) + \eta_{21}q_2^3(t)\right.\\&\left.+s_{11}q_1(t)q_2^2(t) + s_{12}q_1^2(t)q_2(t)\right]\end{aligned} \tag{10a}$$

$$\begin{aligned}&\ddot{q}_2(t) + \omega_2^2 q_2(t) = -\varepsilon g_2^2 q_1(t) + \varepsilon c_{22}\dot{q}_2(t)\\&+\varepsilon c_{12}\dot{q}_1(t) + \varepsilon\left[\eta_{22}q_2^3(t) + \eta_{12}q_1^3(t)\right.\\&\left.+s_{22}q_1^2(t)q_2(t) + s_{21}q_1(t)q_2^2(t)\right]\end{aligned} \tag{10b}$$

where ε is a small parameter, $q_n = \frac{P_n}{h}$,

$A_{ni} = \int_0^a X_n X_i \mathrm{d}x$, $B_{ni} = \int_0^a \left(\frac{\mathrm{d}X_n}{\mathrm{d}x}\right)^2 X_n X_i \mathrm{d}x$,

$C_{ni} = \int_0^a \frac{\mathrm{d}^2 X_n}{\mathrm{d}x^2} X_i \mathrm{d}x$, $D_{ni} = \int_0^a X_n^2 \frac{\mathrm{d}^2 X_n}{\mathrm{d}x^2} X_i \mathrm{d}x$,

$F_{ni} = \int_0^a \left(\frac{\mathrm{d}X_n}{\mathrm{d}x}\right)^2 \frac{\mathrm{d}^2 X_n}{\mathrm{d}x^2} X_i \mathrm{d}x$, $H_{ni} = \int_0^a X_n^3 X_i \mathrm{d}x$,

$M_{ni} = \int_0^a \frac{\mathrm{d}^4 X_n}{\mathrm{d}x^4} X_i \mathrm{d}x$, $Q_{1i} = \int_0^a X_1^2 X_2 X_i \mathrm{d}x$,

$Q_{2i} = \int_0^a X_1 X_2^2 X_i \mathrm{d}x$, $S_{1i} = \int_0^a X_1 \left(\frac{\mathrm{d}X_2}{\mathrm{d}x}\right)^2 X_i \mathrm{d}x$,

$S_{2i} = \int_0^a \frac{\mathrm{d}^2 X_1}{\mathrm{d}x^2} X_2^2 X_i \mathrm{d}x$, $S_{3i} = \int_0^a \frac{\mathrm{d}^2 X_1}{\mathrm{d}x^2} \left(\frac{\mathrm{d}X_2}{\mathrm{d}x}\right)^2 X_i \mathrm{d}x$,

$S_{4i} = \int_0^a \left(\frac{\mathrm{d}X_1}{\mathrm{d}x}\right)^2 X_2 X_i \mathrm{d}x$, $S_{5i} = \int_0^a X_1^2 \frac{\mathrm{d}^2 X_2}{\mathrm{d}x^2} X_i \mathrm{d}x$,

$S_{6i} = \int_0^a \left(\frac{\mathrm{d}X_1}{\mathrm{d}x}\right)^2 \frac{\mathrm{d}^2 X_2}{\mathrm{d}x^2} X_i \mathrm{d}x$, $K_{1i} = \int_0^a \frac{\mathrm{d}X_1}{\mathrm{d}x}\frac{\mathrm{d}X_2}{\mathrm{d}x} X_2 X_i \mathrm{d}x$,

$K_{2i} = \int_0^a X_1 X_2 \frac{\mathrm{d}^2 X_2}{\mathrm{d}x^2} X_i \mathrm{d}x$,

$K_{3i} = \int_0^a \frac{\mathrm{d}X_1}{\mathrm{d}x}\frac{\mathrm{d}X_2}{\mathrm{d}x}\frac{\mathrm{d}^2 X_2}{\mathrm{d}x^2} X_i \mathrm{d}x$,

$K_{4i} = \int_0^a X_1 \frac{\mathrm{d}X_1}{\mathrm{d}x}\frac{\mathrm{d}X_2}{\mathrm{d}x} X_i \mathrm{d}x$, $K_{5i} = \int_0^a X_1 X_2 \frac{\mathrm{d}^2 X_1}{\mathrm{d}x^2} X_i \mathrm{d}x$,

$K_{6i} = \int_0^a \frac{\mathrm{d}X_1}{\mathrm{d}x}\frac{\mathrm{d}X_2}{\mathrm{d}x}\frac{\mathrm{d}^2 X_1}{\mathrm{d}x^2} X_i \mathrm{d}x$,

$\omega_1^2 = \frac{D_M M_{11}}{\rho h A_{11}} - \frac{2\pi^2 D_M C_{11}}{\rho h b^2 A_{11}} + \frac{\pi^4 D_M}{b^4 \rho h}$,

$\omega_2^2 = \frac{D_M M_{22}}{\rho h A_{22}} - \frac{2\pi^2 D_M C_{22}}{\rho h b^2 A_{22}} + \frac{\pi^4 D_M}{b^4 \rho h}$,

$c_{11} = \frac{\sigma h^2 B_{0z}^2}{12\rho\varepsilon}\left(\frac{C_{11}}{A_{11}} - \frac{\pi^2}{b^2}\right)$, $c_{21} = \frac{\sigma h^2 B_{0z}^2 C_{21}}{12\rho A_{11}\varepsilon}$,

$c_{12} = \frac{\sigma h^2 B_{0z}^2 C_{12}}{12\rho A_{22}\varepsilon}$, $c_{22} = \frac{\sigma h^2 B_{0z}^2}{12\rho\varepsilon}\left(\frac{C_{22}}{A_{22}} - \frac{\pi^2}{b^2}\right)$,

$g_1^2 = \frac{D_M M_{21}}{\rho h A_{11}\varepsilon} - \frac{2\pi^2 D_M C_{21}}{\rho h b^2 A_{11}\varepsilon} + \frac{\pi^4 D_M A_{21}}{b^4 \rho h A_{11}\varepsilon}$,

$g_2^2 = \frac{D_M M_{12}}{\rho h A_{22}\varepsilon} - \frac{2\pi^2 D_M C_{12}}{\rho h b^2 A_{22}\varepsilon} + \frac{\pi^4 D_M A_{12}}{b^4 \rho h A_{22}\varepsilon}$, $a_{i1} = \frac{3\pi^2 h D_N}{8\rho b^2 A_{ii}\varepsilon}$,

$a_{i2} = \frac{\pi^2 h D_N}{8\rho b^2 A_{ii}\varepsilon}$, $a_{i3} = \frac{9 h D_N}{8\rho A_{ii}\varepsilon}$, $a_{i4} = \frac{3 h D_N}{8\rho A_{ii}\varepsilon}\left(\frac{\pi}{b}\right)^4$,

$\eta_{ni} = a_{i1}B_{ni} + a_{i2}D_{ni} + a_{i3}F_{ni} - a_{i4}H_{ni}$,

$s_{i1} = a_{i1}(S_{1i} + 2K_{1i}) + a_{i2}(S_{2i} + 2K_{2i}) + a_{i3}(S_{3i} + 2K_{3i}) - 3a_{i4}Q_{1i}$,

$s_{i2} = a_{i1}(S_{4i} + 2K_{4i}) + a_{i2}(S_{5i} + 2K_{5i}) + a_{i3}(S_{6i} + 2K_{6i}) - 3a_{i4}Q_{2i}$ $(i = 1,2;\ n = 1,2)$.

3.2 Method of Multiple Scales

We seek an approximate solution of Eq. (10a) and Eq. (10b) for small but finite amplitudes in the form [25]

$$q_1 = q_{11}(T_0, T_1) + \varepsilon q_{12}(T_0, T_1) \tag{11a}$$

https://doi.org/10.1017/jmech.2017.30 Published online by Cambridge University Press

$$q_2 = q_{21}(T_0, T_1) + \varepsilon q_{23}(T_0, T_1) \tag{11b}$$

where the time scales $T_n = \varepsilon^n t$.

Then substituting Eq. (11a), Eq. (11b) into Eq. (10a), Eq. (10b) and equating the coefficients of like powers of ε, we obtain

Order ε^0

$$D_0^2 q_{11} + \omega_1^2 q_{11} = 0 \tag{12a}$$

$$D_0^2 q_{21} + \omega_2^2 q_{21} = 0 \tag{12b}$$

Order ε^1

$$\begin{aligned} &D_0^2 q_{12} + \omega_1^2 q_{12} = -2D_0 D_1 q_{11} - g_1^2 q_{21} + c_{11} D_0 q_{11} \\ &+c_{21} D_0 q_{21} + \left(\eta_{11} q_{11}^3 + \eta_{21} q_{21}^3 + s_{11} q_{11} q_{21}^2 + s_{12} q_{21} q_{11}^2\right) \end{aligned} \tag{12c}$$

$$\begin{aligned} &D_0^2 q_{22} + \omega_2^2 q_{22} = -2D_0 D_1 q_{21} - g_2^2 q_{11} + c_{22} D_0 q_{21} \\ &+c_{12} D_0 q_{11} + \left(\eta_{22} q_{21}^3 + \eta_{12} q_{11}^3 + s_{21} q_{11} q_{21}^2 + s_{22} q_{21} q_{11}^2\right) \end{aligned} \tag{12d}$$

where $D_0 = \dfrac{\partial}{\partial T_0}$, $D_1 = \dfrac{\partial}{\partial T_1}$, $D_0^2 = \dfrac{\partial^2}{\partial T_0^2}$.

The solutions of Eq. (12a) and Eq. (12b) can be written in the form [25]

$$q_{11} = A_1(T_1) e^{\mathrm{i}\omega_1 T_0} + \overline{A}_1(T_1) e^{-\mathrm{i}\omega_1 T_0} \tag{13a}$$

$$q_{21} = A_2(T_1) e^{\mathrm{i}\omega_2 T_0} + \overline{A}_2(T_1) e^{-\mathrm{i}\omega_2 T_0} \tag{13b}$$

Substituting Eq. (13a), Eq. (13b) into Eq. (12c), Eq. (12d) yields

$$\begin{aligned} &D_0^2 q_{12} + \omega_1^2 q_{12} = \left(-2\mathrm{i}\omega_1 A_1' + c_{11}\mathrm{i}\omega_1 A_1 + 3\eta_{11} A_1^2 \overline{A}_1\right. \\ &\left.+2s_{11} A_1 A_2 \overline{A}_2\right) e^{\mathrm{i}\omega_1 T_0} + \left(c_{21}\mathrm{i}\omega_2 A_2 - g_1^2 A_2 + 3\eta_{21} A_2^2 \overline{A}_2\right. \\ &\left.+2s_{12} A_1 \overline{A}_1 A_2\right) e^{\mathrm{i}\omega_2 T_0} + \eta_{11} A_1^3 e^{3\mathrm{i}\omega_1 T_0} + \eta_{21} A_2^3 e^{3\mathrm{i}\omega_2 T_0} \\ &+s_{11} A_1 A_2^2 e^{\mathrm{i}(\omega_1 + 2\omega_2) T_0} + s_{12} A_1^2 A_2 e^{\mathrm{i}(2\omega_1 + \omega_2) T_0} \\ &+s_{11} A_1 \overline{A}_2^2 e^{\mathrm{i}(\omega_1 - 2\omega_2) T_0} + s_{12} \overline{A}_1^2 A_2 e^{\mathrm{i}(\omega_2 - 2\omega_1) T_0} + cc \end{aligned} \tag{14a}$$

$$\begin{aligned} &D_0^2 q_{22} + \omega_2^2 q_{22} = \left(-2\mathrm{i}\omega_2 A_2' + c_{22}\mathrm{i}\omega_2 A_2 + 3\eta_{22} A_2^2 \overline{A}_2\right. \\ &\left.+2s_{22} A_1 \overline{A}_1 A_2\right) e^{\mathrm{i}\omega_2 T_0} + \left(c_{12}\mathrm{i}\omega_1 A_1 - g_2^2 A_1 + 3\eta_{12} A_1^2 \overline{A}_1\right. \\ &\left.+2s_{21} A_1 A_2 \overline{A}_2\right) e^{\mathrm{i}\omega_1 T_0} + \eta_{22} A_2^3 e^{3\mathrm{i}\omega_2 T_0} + \eta_{12} A_1^3 e^{3\mathrm{i}\omega_1 T_0} \\ &+s_{21} A_1 A_2^2 e^{\mathrm{i}(\omega_1 + 2\omega_2) T_0} + s_{22} A_1^2 A_2 e^{\mathrm{i}(2\omega_1 + \omega_2) T_0} \\ &+s_{21} A_1 \overline{A}_2^2 e^{\mathrm{i}(\omega_1 - 2\omega_2) T_0} + s_{22} \overline{A}_1^2 A_2 e^{\mathrm{i}(\omega_2 - 2\omega_1) T_0} + cc \end{aligned} \tag{14b}$$

where the primes denote differentiation with respect to T_1, and *cc* stands for the complex conjugate of the preceding terms.

3.3 The Internal Resonance Case

The different size ratios of rectangular plate can result in different proportions between the natural frequencies of the first and the second modal. The 1:1 or 1:3 internal resonances will occur when the proportions between the natural frequencies of the first and the second modal satisfy the relationships as $\omega_2 \approx \omega_1$ or $\omega_2 \approx 3\omega_1$. These two internal resonances will be discussed as follows.

3.3.1 One-to-One (1:1) Internal Resonance

We consider the first case, namely $\omega_2 \approx \omega_1$. To express quantitatively the nearness of ω_2 andω_1, here we introduce a detuning parameter δ_1 and let

$$\omega_2 = \omega_1 + \varepsilon\delta_1$$

And then

$$\omega_2 T_0 = \omega_1 T_0 + \varepsilon\delta T_0 = \omega_1 T_0 + \delta_1 T_1 \tag{15}$$

Inspection of the right-hand sides of Eq. (14a) and Eq. (14b) reveals that in addition to the terms proportional to $e^{\pm\mathrm{i}\omega_n T_0}$ secular terms are produced by the terms proportional to $e^{\pm\mathrm{i}\omega_1 T_0}$ in Eq. (14a) and the terms proportional to $e^{\pm\mathrm{i}\omega_1 T_0}$ in Eq. (14b). In order to show this secular behavior we express these factors as

$$e^{\pm\mathrm{i}\omega_2 T_0} = e^{\pm\mathrm{i}\omega_1 T_0 \pm \mathrm{i}\delta_1 T_1}, \quad e^{\pm\mathrm{i}\omega_1 T_0} = e^{\pm\mathrm{i}\omega_2 T_0 \mp \mathrm{i}\delta_1 T_1}$$

Then the secular terms are eliminated from q_{13} and q_{23} if

$$\begin{aligned} &-2\mathrm{i}\omega_1 A_1' + c_{11}\mathrm{i}\omega_1 A_1 + 3\eta_{11} A_1^2 \overline{A}_1 + 2s_{11} A_1 A_2 \overline{A}_2 \\ &+(c_{21}\mathrm{i}\omega_2 A_2 - g_1^2 A_2 + 3\eta_{21} \overline{A}_2 A_2^2 + 2s_{12} A_1 \overline{A}_1 A_2) e^{\mathrm{i}\delta_1 T_1} = 0 \end{aligned} \tag{16a}$$

$$\begin{aligned} &-2\mathrm{i}\omega_2 A_2' + c_{22}\mathrm{i}\omega_2 A_2 + 3\eta_{22} A_2^2 \overline{A}_2 + 2s_{22} A_1 \overline{A}_1 A_2 \\ &+(c_{12}\mathrm{i}\omega_1 A_1 - g_2^2 A_1 + 3\eta_{12} A_1^2 \overline{A}_1 + 2\mathrm{s}_{21} A_1 A_2 \overline{A}_2) e^{-\mathrm{i}\delta_1 T_1} = 0 \end{aligned} \tag{16b}$$

We introduce the polar transformation in order to solve Eq. (16a) and Eq. (16b)

$$A_m = \frac{1}{2} a_m(T_1) e^{\mathrm{i}\theta_m(T_1)} \quad (m = 1, 2) \tag{17}$$

where $a_m(T_1)$ and $\theta_m(T_1)$ are the amplitude and phase of *m*th mode.

Substituting Eq. (17) into Eq. (16a) and Eq. (16b), and separating real and imaginary parts, we obtain the modulation equations

$$\begin{aligned} 8\omega_1 a_1' &= 4\omega_1 c_{11} a_1 - (4g_1^2 a_2 - 3\eta_{21} a_2^3 - 2s_{12} a_1^2 a_2)\sin\gamma_1 \\ &+4c_{21}\omega_2 a_2 \cos\gamma_1 \end{aligned} \tag{18a}$$

$$\begin{aligned} 8\omega_2 a_2' &= 4\omega_2 c_{22} a_2 + (4g_2^2 a_1 - 3\eta_{12} a_1^3 - 2s_{21} a_1 a_2^2)\sin\gamma_1 \\ &+4c_{12}\omega_1 a_1 \cos\gamma_1 \end{aligned} \tag{18b}$$

$$\begin{aligned} 8\omega_1 a_1 \theta_1' &= -3\eta_{11} a_1^3 - 2s_{11} a_1 a_2^2 + 4c_{21}\omega_2 a_2 \sin\gamma_1 \\ &+(4g_1^2 a_2 + 3\eta_{21} a_2^3 + 2s_{12} a_1^2 a_2)\cos\gamma_1 \end{aligned} \tag{18c}$$

https://doi.org/10.1017/jmech.2017.30 Published online by Cambridge University Press

$$8\omega_2 a_2\theta_2' = -3\eta_{22}a_2^3 - 2s_{22}a_1^2a_2 - 4c_{12}\omega_1 a_1\sin\gamma_1 + (4g_2^2a_1 + 3\eta_{12}a_1^3 + 2s_{21}a_1a_2^2)\cos\gamma_1 \quad (18d)$$

where $\gamma_1 = \theta_2 - 3\theta_1 + \delta_1 T_1$.

Eliminating θ_1 and θ_2 from Eq. (18c) through Eq. (18d) yields

$$a_2\gamma_1' = a_2\delta_1 + \left(\frac{s_{11}}{4\omega_1} - \frac{3\eta_{22}}{8\omega_2}\right)a_2^3 + \left(\frac{3\eta_{11}}{8\omega_1} - \frac{s_{22}}{4\omega_2}\right)a_1^2a_2 + \left(\frac{c_{12}\omega_1 a_1}{2\omega_2} + \frac{c_{21}\omega_2 a_2^2}{2\omega_1 a_1}\right)\sin\gamma_1 + \left(\frac{g_2^2a_1}{2\omega_2} - \frac{g_1^2a_2^2}{2\omega_1} + \frac{3\eta_{12}a_1^3}{8\omega_2} - \frac{3\eta_{21}a_2^4}{8\omega_1 a_1} + \frac{s_{21}a_1a_2^2}{4\omega_2} - \frac{s_{12}a_1a_2^2}{4\omega_1}\right)\cos\gamma_1 \quad (19)$$

3.3.2 One-to-Three (1:3) Internal Resonance

Then we consider the second case, namely $\omega_2 \approx 3\omega_1$. To express quantitatively the nearness of ω_2 and $3\omega_1$, we introduce a detuning parameter δ_2 according to

$$\omega_2 = 3\omega_1 + \varepsilon\delta_2$$

Inspection of the right-hand sides of Eq. (14a) and Eq. (14b) reveals that in addition to the terms proportional to $e^{\pm i\omega_1 T_0}$ secular terms are produced by the terms proportional to $e^{\pm i(\omega_2 - 2\omega_1)T_0}$ in Eq. (14a) and the terms proportional to $e^{\pm 3i\omega_1 T_0}$ in Eq. (14b).

The secular terms are eliminated from q_{13} and q_{23} if

$$-2i\omega_1 A_1' + c_{11}i\omega_1 A_1 + 3\eta_{11}A_1^2\bar{A}_1 + 2s_{11}A_1A_2\bar{A}_2 + s_{12}\bar{A}_1^2A_2e^{i\delta_2 T_1} = 0 \quad (20a)$$

$$-2i\omega_2 A_2' + c_{22}i\omega_2 A_2 + 3\eta_{22}A_2^2\bar{A}_2 + 2s_{22}A_1\bar{A}_1A_2 + \eta_{12}A_1^3e^{-i\delta_2 T_1} = 0 \quad (20b)$$

Substituting Eq. (17) in Eq. (20a), Eq. (20b) and separating real and imaginary parts, we also obtain the modulation equations

$$8\omega_1 a_1' = 4\omega_1 c_{11}a_1 + s_{12}a_1^2a_2\sin\gamma_2 \quad (21a)$$

$$8\omega_2 a_2' = 4\omega_2 c_{22}a_2 - \eta_{12}a_1^3\sin\gamma_2 \quad (21b)$$

$$8\omega_1 a_1\theta_1' = -\left(3\eta_{11}a_1^2 + 2s_{11}a_2^2\right)a_1 - s_{12}a_1^2a_2\cos\gamma_2 \quad (21c)$$

$$8\omega_2 a_2\theta_2' = -\left(3\eta_{22}a_2^2 + 2s_{12}a_1^2\right)a_2 - \eta_{12}a_1^3\cos\gamma_2 \quad (21d)$$

where $\gamma_2 = \theta_2 - 3\theta_1 + \delta_2 T_1$.

Then, eliminating θ_1 and θ_2 from Eq. (21c) through Eq. (21d) yields

$$a_2\gamma_2' = a_2\delta_2 + \left(\frac{3s_{11}}{4\omega_1} - \frac{3\eta_{22}}{8\omega_2}\right)a_2^3 + \left(\frac{9\eta_{11}}{8\omega_1} - \frac{s_{22}}{4\omega_2}\right)a_1^2a_2 + \left(\frac{3s_{12}a_1a_2^2}{8\omega_1} - \frac{\eta_{12}a_1^3}{8\omega_2}\right)\cos\gamma_2 \quad (22)$$

Thus the problem is reduced to finding the solutions of simultaneous Eqs (18a), (18b), (19) and Eqs (21a), (21b), (22).

4. THE ANALYSIS OF NUMERICAL RESULTS

Considering the rectangular aluminum thin plate in constant transverse magnetic field, Fig. 2 shows the relationship between ω_2/ω_1 representing the natural frequency ratio of the first two modes and b/a representing the size ratio of the rectangular plate when the thin plate is in free vibration. It can also be seen from the figure that when the size ratio of rectangular plate is approximately less than 0.3, one-to-one (1:1) internal resonance will happen, and if the size ratio is approximately greater than 1.6, one-to-three (1:3) internal resonance is said to take place. Consequently we can analyze different internal resonance cases by adjusting the size of the plate.

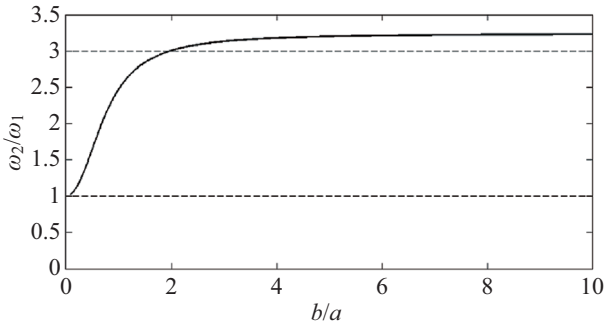


Fig. 2 The ω_2/ω_1 ratio versus b/a curve of rectangular plate.

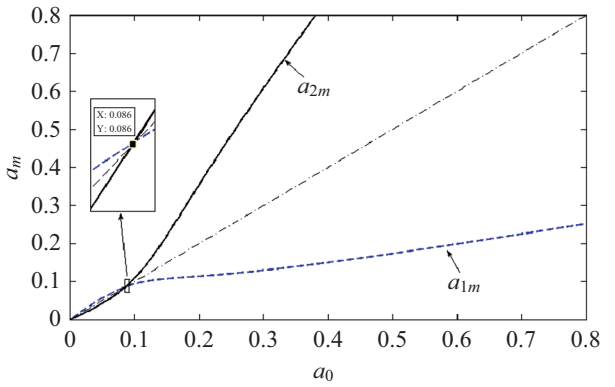


Fig. 3 The curve of amplitude values of modal amplitude and initial values.

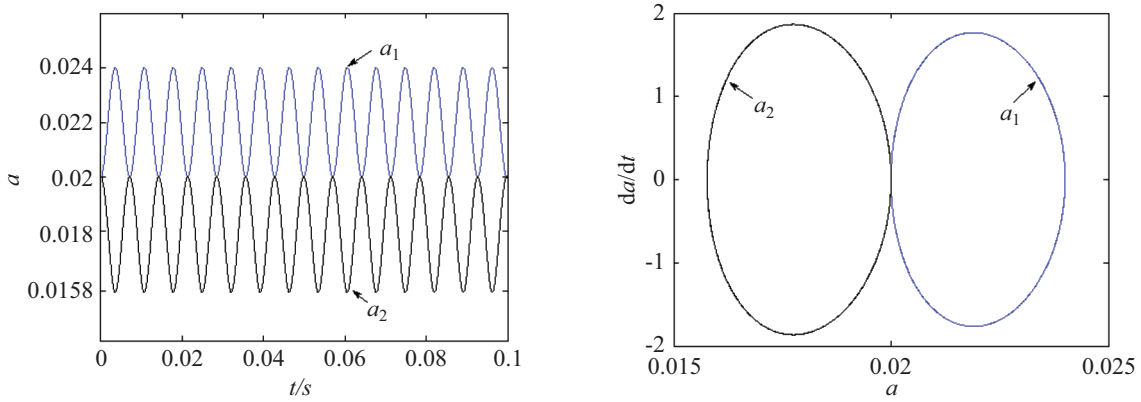
The main parameters of the aluminum thin plate are given as follows: electrical conductivity is $\sigma = 3.63 \times 10^7(\Omega\cdot m)^{-1}$, the density is $\rho = 2670$ kg/m^3, the Poisson's ratio is $\nu = 0.34$, Young's modulus is $E = 71$ Gpa, the thickness is $h = 6$ mm. When considering the case of 1:1 internal resonance we let $a = 0.6$ m, $b = 0.15$ m, the natural frequencies of the first two modes are approximately $\omega_1 = 4478.1$ *rad/s*, $\omega_2 = 5340$ *rad/s*. When considering the case of 1:3 internal resonance we let $a = 0.6$ m, $b = 1.2$ m, the natural frequencies of the first two modes are approximately $\omega_1 = 457.5$ *rad/s*, $\omega_2 = 1374.5$ *rad/s*.

The following is mainly concerned about the 1:1 resonance characteristics of the system.

https://doi.org/10.1017/jmech.2017.30 Published online by Cambridge University Press

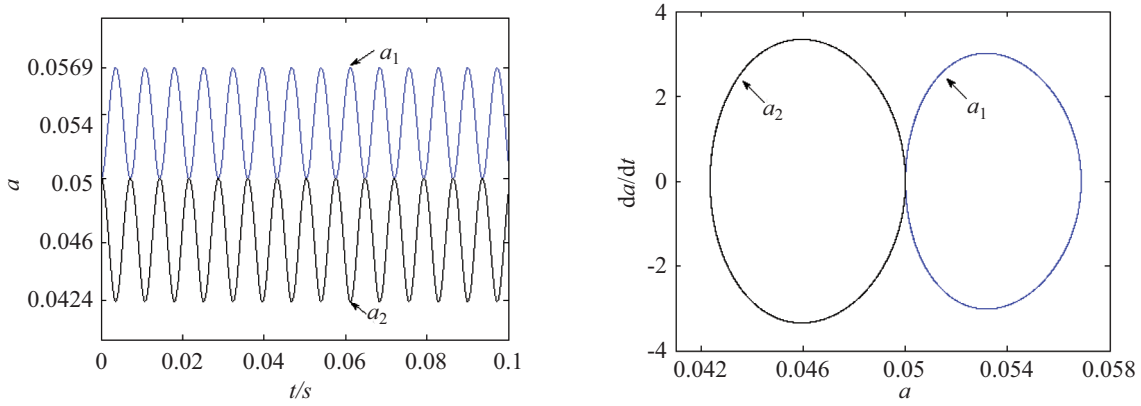
4.1 In the Absence of Damping

The system exhibits free oscillation when the magnetic field intensity is zero thus magnetic damping is absent. Figure 3 is the variation of amplitude values of



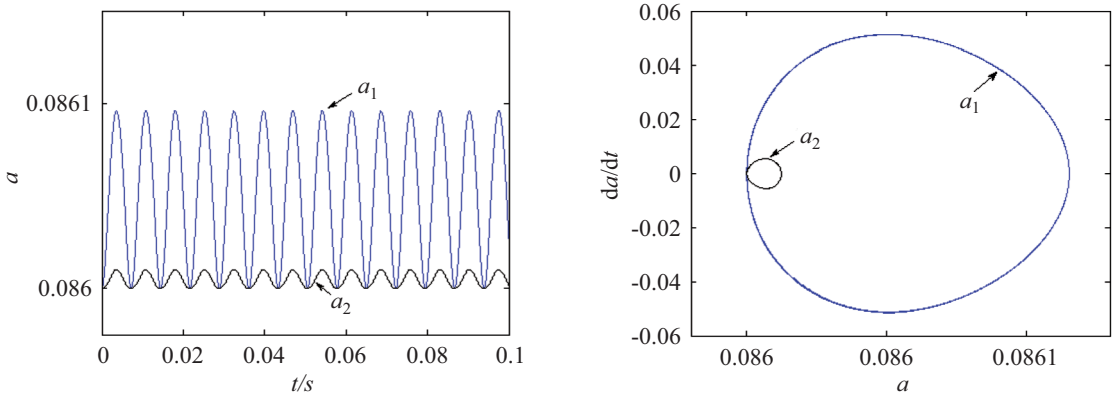
(a) The time history response diagrams (b) The phase portraits

Fig. 4 The internal resonance response diagram of system (the initial values are $a_{10} = a_{20} = 0.02$).



(a) The time history response diagrams (b) The phase portraits

Fig. 5 The internal resonance response diagram of system (the initial values are $a_{10} = a_{20} = 0.05$).



(a) The time history response diagrams (b) The phase portraits

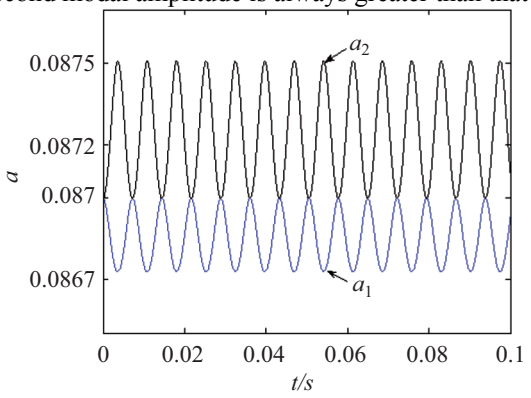
Fig. 6 The internal resonance response diagram of system (the initial values are $a_{10} = a_{20} = 0.086$).

the first and second modal amplitude under different initial conditions, which shows that the amplitude value of the first modal amplitude is always greater than that of the second modal amplitude when the initial value is less than 0.086. In terms of the given initial value (the dash-dot line as shown in Fig. 3) as wave center, the relative amplitude is approximately equal to each other for the two modes. With the increase of the initial value, the relative amplitude increases first and then decreases. When the initial value is greater than 0.086, the ampli-

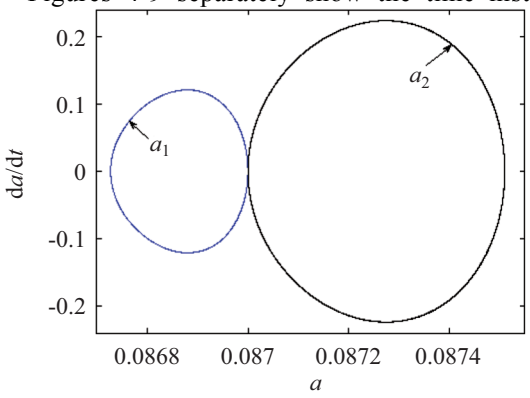
https://doi.org/10.1017/jmech.2017.30 Published online by Cambridge University Press

tude of the second modal amplitude exceeds that of the first modal amplitude. Moreover, the relative amplitude of the second modal amplitude is always greater than that of the first one, and both grow with the increase of initial value.

Figures 4-9 separately show the time history re-

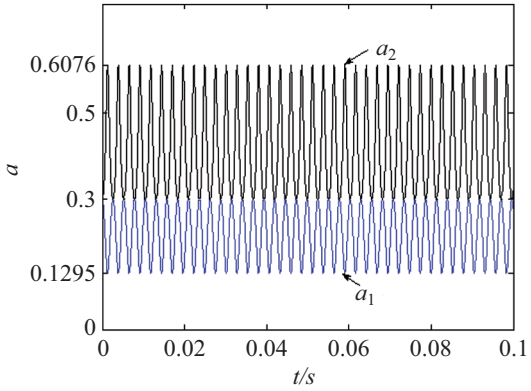


(a) The time history response diagrams

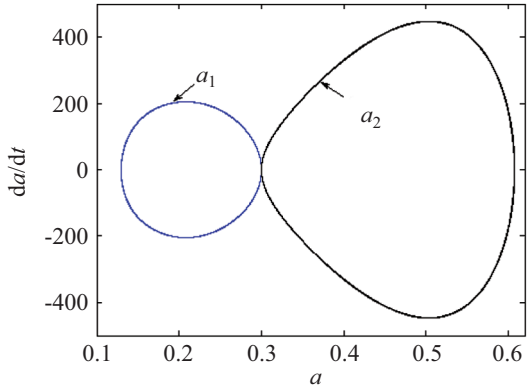


(b) The phase portraits

Fig. 7 The internal resonance response diagram of system (the initial values are $a_{10} = a_{20} = 0.087$).

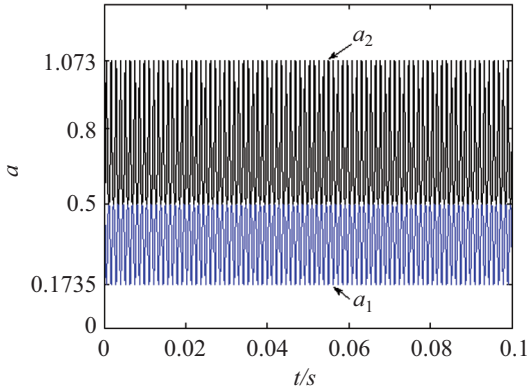


(a) The time history response diagrams

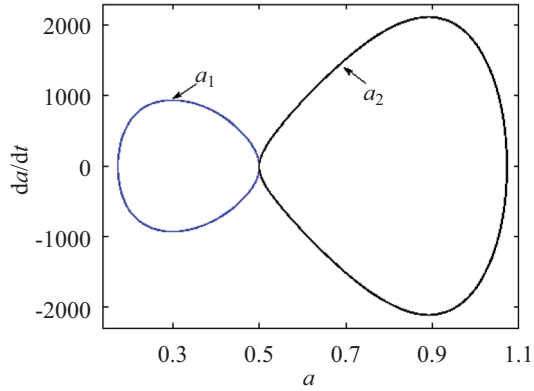


(b) The phase portraits

Fig. 8 The internal resonance response diagram of system (the initial values are $a_{10} = a_{20} = 0.3$).



(a) The time history response diagrams



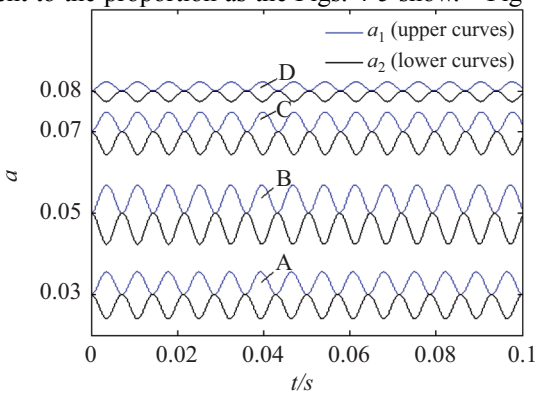
(b) The phase portraits

Fig. 9 The internal resonance response diagram of system (the initial values are $a_{10} = a_{20} = 0.5$).

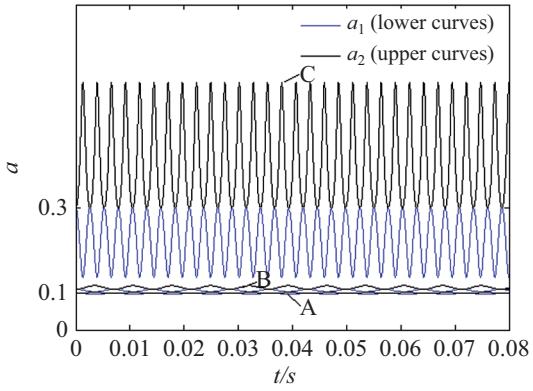
sponses of non-dimensional modal amplitude and the phase of amplitude under different initial conditions. The energy of the system continues to be exchanged undamped between the two modes of oscillation as shown in time history responses. It illustrates that the system exhibits an obvious 1:1 internal resonance. The phase portraits present two closed curves, which indicate that the system presents a stable single periodic motion. The vibration of the system changes with the initial values that when the initial values are less than 0.086, the relative amplitude of the first and second modal amplitudes are approximately equal and the phase portraits are

https://doi.org/10.1017/jmech.2017.30 Published online by Cambridge University Press

two closed circular rings of approximately equal sizes, which means energy in the first and the second mode is equivalent to the proportion as the Figs. 4-5 show. Figure 6 shows that when the initial value is 0.086, the relative amplitudes of the first and second mode amplitudes are close to zero. That is to say the energy exchanged

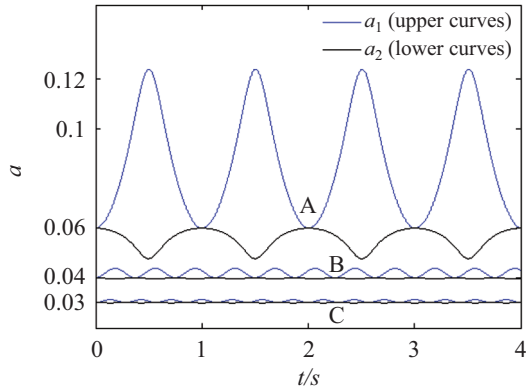


(a) The initial values are less than 0.086

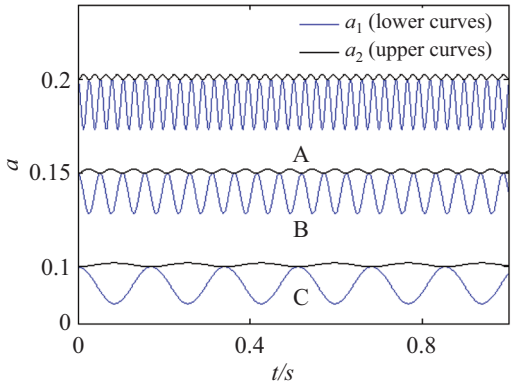


(b) The initial values are more than 0.086

Fig. 10 The modal amplitude time history diagram under different initial conditions.



(a) The initial values are less than 0.071



(b) The initial values are more than 0.071

Fig. 11 The modal amplitude time history diagram under different initial conditions in 1:3 internal resonance.

between the two modes is minimum and the internal resonance phenomenon is the least obvious. When the initial value reaches 0.087, the second modal amplitude exceeds the first modal amplitude and the closed circular ring representing the second mode is also switched to the right in the phase portrait. When the initial value is greater than 0.087, the relative amplitude value of the second modal amplitude is always greater than that of the first modal amplitude and the energy is mainly distributed in the second mode. As shown above, the internal resonance is very sensitive to the initial values, which reflects the nonlinear vibration characteristics of internal resonance.

Figure 10(a) shows four sets of curves A, B, C and D which respectively represents the amplitude time history diagrams of the first mode (upper curves)and the second mode (lower curves) under the initial values of 0.03, 0.05, 0.07 and 0.08, and three sets of curves A,B and C respectively representing the amplitude time history diagrams of the first mode (lower curves)and the second mode (upper curves) under the initial values of 0.09, 0.1 and 0.3 are shown in Fig. 10(b). Investigating the figures, we find out that the amplitude values of the first and second modal amplitudes increase first and then decrease with the growth of the initial value, but the vibration frequency keeps constant when the initial value is less than the critical value 0.086. When the initial value exceeds the critical value 0.086, the amplitude value and vibration frequency both rise with the increase of initial value.

As a contrast, Figs. 11(a) and (b) are two groups of modal amplitude time history diagrams under different initial conditions in 1:3 internal resonance. Figure 11(a) shows three sets of curves A, B and C which respectively represent the amplitude time history diagrams of the first mode (upper curves) and the second mode (lower curves) under the initial values of 0.03, 0.04 and 0.06, and three sets of curves A, B and C representing the amplitude time history diagrams of the first mode (lower curves) and the second mode (upper curves) under the initial values of 0.1, 0.15 and 0.2 are shown in Fig. 11(b). It is indicated that the amplitude values of the first and second modal amplitudes increase and the vibration frequency decreases with the rise of the initial value when the initial value is less than 0.071 (the critical value of 1:3 internal resonance). When the initial value is greater than the critical value 0.071, with the increase of initial value, the vibration frequency grows.

Figure 12 shows the modal amplitude history dia-

https://doi.org/10.1017/jmech.2017.30 Published online by Cambridge University Press

grams under different plate thickness for h = 5 mm, h = 6 mm, h = 7 mm with initial value for $a_{10} = a_{20} = 0.1$. The upper curves represent the amplitude of the second mode and the lower curves for the first mode. It can be seen that the change of the plate thickness does not affect the internal resonance characteristics of the system, and

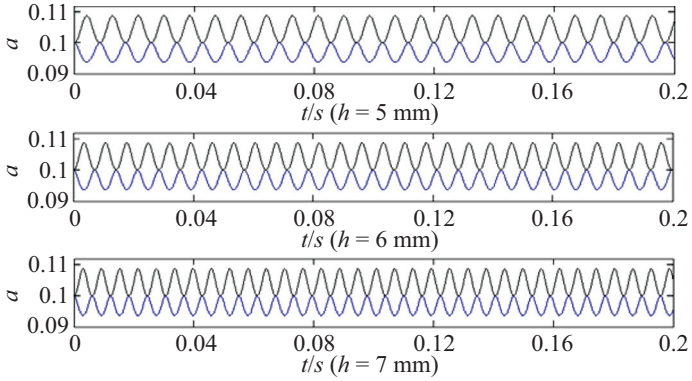
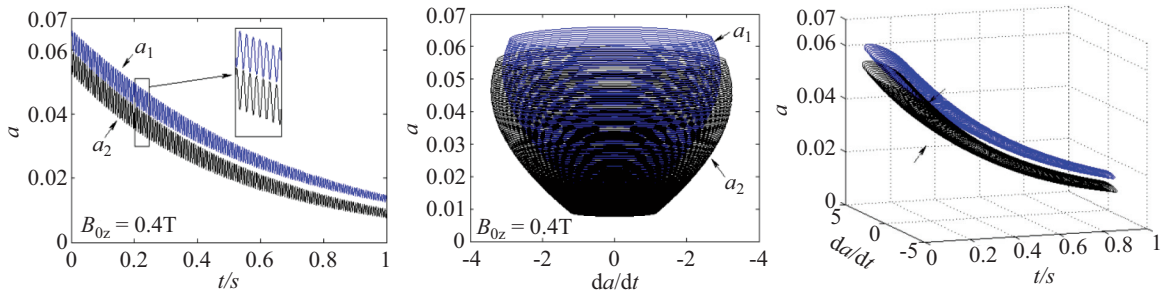
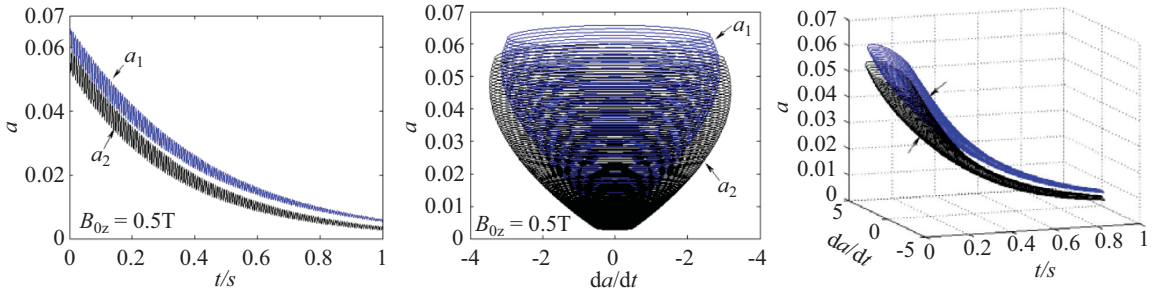


Fig. 12 The modal amplitude time history diagrams under different thickness of the plate.



(a) The time history response diagrams (b) The phase portraits (c) The 3D response diagram

Fig. 13 The internal resonance response diagram of system (B_{0z} = 0.4T).



(a) The time history response diagrams (b) The phase portraits (c) The 3D response diagram

Fig. 14 The internal resonance response diagram of system (B_{0z} = 0.5T).

nor does it affect the modal amplitude value of the first or the second mode, whereas the vibration frequency of the system increases with the growth of the thickness of plate.

4.2 In the Presence of Damping

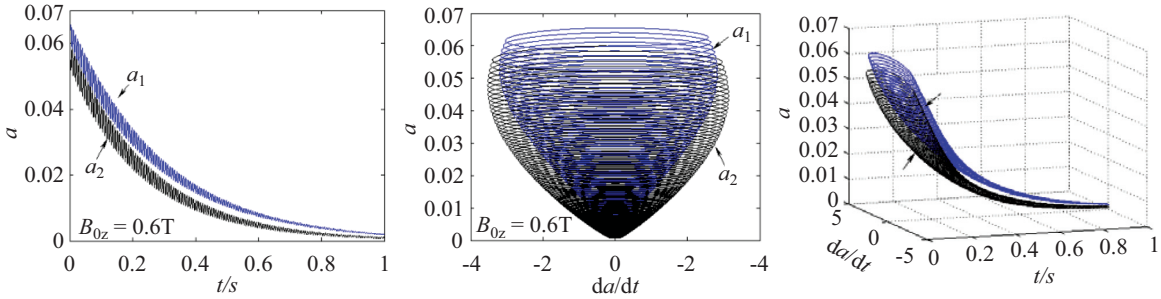
Considering a system in magnetic field in this case, the damping term is determined by the intensity of the magnetic field. We discuss the effects of the magnetic field intensity on the modal amplitude in the case of internal resonance.

By setting the same initial value for $a_{10} = a_{20} = 0.06$, the time history diagrams, phase portraits of two modal amplitudes and 3-dimensional curves of time, modal amplitude and modal amplitude velocity under the different magnetic intensities for B_{0z} = 0.4T, B_{0z} = 0.5T, B_{0z} = 0.6T are shown in Figs. 13-15. We can see that because of the existence of internal resonance, the modal amplitudes of the first and the second mode are coupled with the damped oscillation and the amplitude of oscillation decreases gradually with magnetic intensity. Furthermore the energy of the system continues to be exchanged between the two modes but it is continuously

https://doi.org/10.1017/jmech.2017.30 Published online by Cambridge University Press

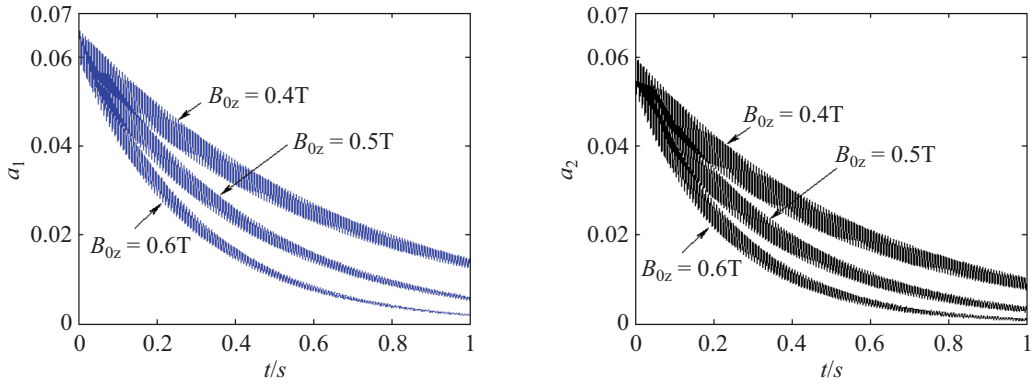
dissipated at the same time.

Figures 16(a) and (b) respectively represents the change of amplitude of the first and the second modes with time under different magnetic field intensities. It can be seen that the external magnetic field poses an obvious inhibiting effect on the modal amplitude. The



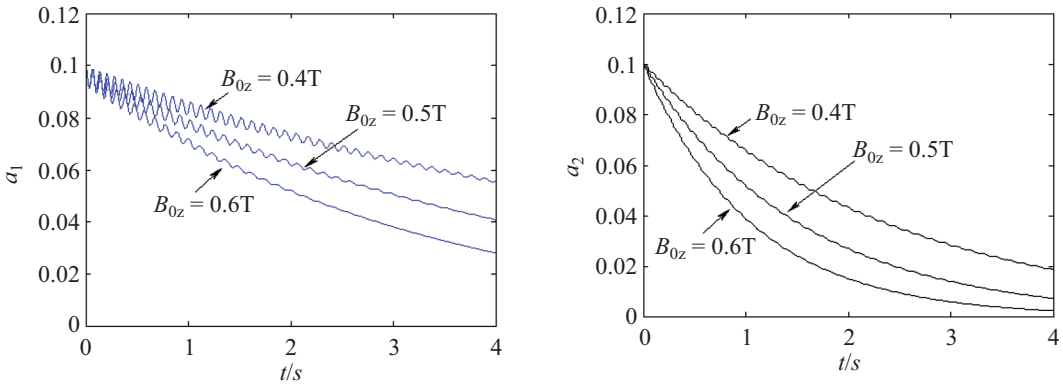
(a) The time history response diagrams (b) The phase portraits (c) The 3D response diagram

Fig. 15 The internal resonance response diagram of system (B_{0z} = 0.6T).



(a) a_1 (a) a_2

Fig. 16 The time history diagram of modal amplitude under different magnetic field intensities (B_{0z} = 0.4T, B_{0z} = 0.5T, B_{0z} = 0.6T).



(a) a_1 (a) a_2

Fig. 17 The time history diagram of modal amplitude under different magnetic field intensities in 1:3 internal resonance (B_{0z} = 0.4T, B_{0z} = 0.5T, B_{0z} = 0.6T).

decay rates of the two modal amplitudes are almost the same and they both increase with the growth of the magnetic field intensity. Furthermore, the greater the magnetic field is, the smaller the oscillation of the modal amplitude is.

On the contrary, Figs. 17(a) and (b) respectively exhibits the change of amplitudes of the two modes with time under different magnetic field intensities in the case of 1:3 internal resonance. The decay rate of the second modal amplitude is faster than that of the first modal amplitude. In the same magnetic field the decay rate of modal amplitude in 1:3 internal resonance is slower than that in 1:1 internal resonance and the energy is mainly distributed in the first mode. The two figures also show

https://doi.org/10.1017/jmech.2017.30 Published online by Cambridge University Press

the similar phenomenon in two cases of internal resonances that the external magnetic field inhibits the modal amplitude, and the decay rates of the two modal amplitudes both grow with the rise of the magnetic field intensity.

4. CONCLUSIONS

Based on Maxwell equations and the theory of elastic dynamics, we deduce the nonlinear magneto elastic vibration differential equations of rectangular conductive thin plate in transverse constant magnetic field. The method of multiple scales has been adopted to obtain the modulation equations of the amplitudes and phase angles via 1:1 or 1:3 internal resonance with different size ratios. The 1:1 internal resonance characteristics of the system are analyzed through a numerical example, and the results are compared with the partial results of 1:3 internal resonance. It can be concluded that:

(1) Different size ratios of rectangular thin plate can make the system exhibit 1:1 or 1:3 internal resonance.

(2) Due to internal resonance, the energy in the system continues to be exchanged between the two modes of oscillation, which shows the clear characteristics of internal resonance.

(3) In the absence of damping, the system presents single stable periodic motion and the changes of initial values significantly affect the oscillation of the two modes, which indicates the nonlinear characteristics of internal resonance. In the presence of damping, the modal amplitudes of the first and the second mode are coupled with the damped oscillation and the decay rate accelerates with the enhancement of the magnetic field intensity. Moreover, the modal amplitude oscillates more and decays faster compared with the case of 1:3 internal resonance.

ACKNOWLEDGEMENTS

The project is supported by the National Natural Science Foundation of China (No.11472239) and the Natural Science Foundation of Hebei Province of China (No.A2015203023).

REFERENCES

1. Ambarcumian, S. A., Bagdasarian, G. E. and Belubekian, M. V., *Magneto-Elastic of Thin Shells and Plates*, Science Press, Moscow (1997) (Text in Russian).
2. Zheng, X.-J., Zhang, J.-P. and Zhou, Y.-H., "Dynamic Stability of a Cantilever Conductive Plate in Transverse Impulsive Magnetic Field," *International Journal of Solids & Structures*, **42**, pp. 2417-2430 (2005).
3. Zheng, X.-J. and Wang, X.-Z., "A Magnetoelastic Theoretical Model for Soft Ferromagnetic Shell in Magnetic Field," *International Journal of Solids & Structures*, **40**, pp. 6897-6912 (2003).
4. Wang, X.-Z. and Lee, J. S., "Dynamic Stability of Ferromagnetic Beam-Plates with Magnetoelastic Interaction and Magnetic Damping in Transverse Magnetic Fields," *Journal of Engineering Mechanics*, **132**, pp. 422-428 (2006).
5. Pratiher, B. and Dwivedy, S. K., "Nonlinear Vibrations and Frequency Response Analysis of a Cantilever Beam Under Periodically Varying Magnetic Field," *Mechanics Based Design of Structures and Machines*, **39**, pp. 378-391 (2011).
6. Baghdasaryan, G. Y., Danoyan, Z. N. and Mikilyan, M. A., "Issues of Dynamics of Conductive Plate in a Longitudinal Magnetic Field," *International Journal of Solids & Structures*, **50**, pp. 3339-3345 (2013).
7. Hu, Y.-D. and Li, J., "Nonlinear Magnetoelastic Vibrating Equations and Resonance Analysis of Current-Conducting Thin Plate," *International Journal of Structural Stability and Dynamics*, **8**, pp. 597-613 (2008).
8. Hu, Y.-D. and Li, J., "The Magneto-Elastic Subharmonic Resonance of Current-Conducting Thin Plate in Magnetic Field," *Journal of Sound and Vibration*, **319**, pp. 1107-1120 (2009).
9. Hu, Y.-D. and Li, J., "Magneto-Elastic Combination Resonances Analysis of Current-Conducting Thin Plate," *Applied Mathematics and Mechanics (English Edition)*, **29**, pp. 1053-1066 (2008).
10. Hu, Y.-D., Hu, P. and Zhang, J.-Z. "Strongly Nonlinear Subharmonic Resonance and Chaotic Motion of Axially Moving Thin Plate in Magnetic Field," *Journal of Computational and Nonlinear Dynamics*, **10**, 021010 (2015).
11. Hu, Y.-D. and Zhang, J.-Z., "Magneto-Thermo-Elastic Coupled Dynamics Equations of Axially Moving Carry Current Plate in Magnetic Field," *Chinese Journal of Theoretical and Applied Mechanics*, **45**, pp. 792-796 (2013).
12. Nayfeh, A. H. and Balachandran, B., "Modal Interactions in Dynamical and Structural Systems," *ASME Applied Mechanics Reviews*, **42**, pp. 175-210 (1989).
13. Witt, A. A. and Gorelik, G. A., "Vibrations of an Elastic Pendulum as an Example of Vibrations of Two Parametrically Coupled Linear Systems," *Journal of Technical Physics*, **3**, pp. 294-307 (1933).
14. Chen, L.-Q., Zhang, G.-C. and Ding, H., "Internal Resonance in Forced Vibration of Coupled Cantilevers Subjected to Magnetic Interaction," *Journal of Sound & Vibration*, **354**, pp. 196-218 (2015).
15. Anlas, G. and Elbeyli, O., "Nonlinear Vibrations of

https://doi.org/10.1017/jmech.2017.30 Published online by Cambridge University Press

a Simply Supported Rectangular Metallic Plate Subjected to Transverse Harmonic Excitation in the Presence of a One-to-One Internal Resonance," *Nonlinear Dynamics*, **30**, pp. 1-28 (2002).

16. Zhang, W. and Zhao, M.-H., "Nonlinear Vibrations of a Composite Laminated Cantilever Rectangular Plate with One-to-One Internal Resonance," *Nonlinear Dynamics*, **70**, pp. 295-313 (2012).
17. Li, B.-S. and Zhang, W., "Global Bifurcations and Multi-Pulse Chaotic Dynamics of Rectangular Thin Plate with One-to-One Internal Resonance," *Applied Mathematics and Mechanics (English Edition)*, **33**, pp. 1115-1128 (2012).
18. Hao, Y.-X., Zhang, W. and Ji, X.-L., "Nonlinear Dynamic Response of Functionally Graded Rectangular Plates under Different Internal Resonances," *Mathematical Problems in Engineering*, **2010**, pp. 242-256 (2010).
19. Rossikhin, Y. A. and Shitikova, M. V., "Analysis of Free Non-Linear Vibrations of a Viscoelastic Plate under the Conditions of Different Internal Resonances," *International Journal of Non-Linear Mechanics*, **41**, pp. 313-325 (2006).
20. Nayfeh, A. H. and Emam, S. A., "Non-Linear Response of Buckled Beams to 1:1 and 3:1 Internal Resonances," *International Journal of Non-Linear Mechanics*, **52**, pp. 12-25 (2013).
21. Sahoo, B., Panda, L. N. and Pohit, G., "Combination, Principal Parametric and Internal Resonances of an Accelerating Beam under Two Frequency Parametric Excitation," *International Journal of Non-Linear Mechanics*, **78**, pp. 35-44 (2015).
22. Tekin, A., OEzkaya, E. and Bagdatlr, S. M., "Three-to-One Internal Resonance in Multiple Stepped Beam Systems," *Applied Mathematics and Mechanics*, **30**, pp. 1131-1142 (2009).
23. Xiong, L.-Y., Zhang, G.-C., Ding, H. and Chen, L.-Q., "Nonlinear Forced Vibration of a Viscoelastic Buckled Beam with 2:1 Internal Resonance," *Mathematical Problems in Engineering*, **178**, pp. 368-381 (2014).
24. Cao, Z.-Y., *Vibration Theory of Plates and Shells*, China Railway Publishing House, Beijing (1983) (Text in Chinese).
25. Nayfeh, A. H. and Mook, D. T., *Nonlinear Oscillations*, John Wiley & Sons, New York (1979).

(Manuscript received December 5, 2016,
accepted for publication March 26, 2017.)

https://doi.org/10.1017/jmech.2017.30 Published online by Cambridge University Press